Article

Effect of Substrate on One-Dimensional Multiferroic Properties

Ivan Maltsev *[ID] and Igor Bychkov *[ID]

Faculty of Physics, Chelyabinsk State University, 454001 Chelyabinsk, Russia
* Correspondence: malts_iv@mail.ru (I.M.); bychkov@csu.ru (I.B.)

Abstract: We present a theoretical study of the substrate influence on the electrical and magnetic properties of a one-dimensional multiferroic. We used a one-dimensional axial next-nearest neighbor Ising model (1D ANNNI model). The effect of the substrate was modeled using the periodic Frenkel–Kontorova potential. It is shown that the periodic potential of the substrate reduces the polarization of the multiferroic at low temperatures. The substrate potential significantly affects the structural changes near the magnetic phase transition temperature.

Keywords: ferromagnetic; thin films; Frenkel–Kontorova potential; computer simulations

1. Introduction

In recent years, composites of ferromagnetic (FM), antiferromagnetic (AFM), and ferroelectric (FE) materials have received considerable attention due to their wide use in spintronic devices. Such heterostructures can be created from bilayers of FM and FE structures, which enable controlling the magnetic and electrical properties by the strain along the surface [1,2]. Reference [3] showed the strong influence of deformations caused by the structural phase transition in the $BaTiO_3$ FE substrate on the magnetic properties of the $La_{0.7}Sr_{0.3}MnO_6$ ferromagnet. The substrate influence can be significant in the boundary layer of the magnet only. Thus, a noticeable change in material properties because of the substrate can be expected for 2D or 1D materials. Thin film is an example of a 2D multiferroic and the Ca_3CoMnO_6 compound is an example of a 1D multiferroic [4].

Ca_3CoMnO_6 has a rhombohedral structure (crystallographic group $R\bar{3}c$), similar to K_4CdCl_6. It contains parallel $CoMnO_6$ chains consisting of an alternating CoO_6 trigonal prism and MnO_6 octahedron along the c axis. Ca^{2+} ions separate the $CoMnO_6$ chains, which form a triangular lattice in the ab plane [4–6]. Ca_3CoMnO_6 belongs to type II multiferroic in Chomsky's classification [7]. The alternation of Co^{2+} and Mn^{4+} ions along the $CoMnO_6$ chain breaks the spatial symmetry, leading to unusual physical properties, such as magnetization tunneling, electric polarization due to magnetostriction [8], magnetoelectric interaction [9], etc.

The ground state of the magnetic lattice is *up–up–down–down* if the competing interactions parameter is $|J_{AF}/J_{FM}| > 1/2$ [10]. The exchange interaction shortens the distances between parallel spins and increases between anti-parallel ones. This leads to the electric polarization appearance in the *up–up–down–down* magnetic structure.

References [11,12] confirmed the occurrence of ferroelectricity as a result of a change in the Co-Mn distances and *up–up–down–down* magnetic ordering with the help of density functional theory and *ab initio* calculation of the electronic structure. Experimental work [13] revealed ferroelectricity in the $Ca_3Co_{2-x}Mn_xO_6$ crystal ($x \approx 0.96$). The authors of [14] presented the original microscopic model of *up–up–down–down* structure formation in type II multiferroics by using the renormalization group method. Subsequent works showed that the long-range spin order is retained only for $Ca_3Co_{1+x}Mn_{1-x}O_6$ [15], while the long-range order disappears and the macroscopic polarization weakens on defect-free Ca_3CoMnO_6 [16]. Reference [17] showed the relaxor nature of the ferroelectric phase transition, which implied the existence of polar nanoregions [18]. The doped $Ca_{2.7}Sr_{0.3}CoMn_{1-x}Fe_xO_6$ compound

demonstrates a rather large magnetoelectric (ME) interaction coefficient at room temperature (about $1.7 \, \text{mV/cm} \cdot \text{Oe}$) and a decrease in the band gap from 2.25 to 1.8 eV [19], which allows its potential application in sensors, filters, and various actuators working in the mid-frequency range.

In this work, we studied the effect of the substrate on the magnetic and electrical properties of a one-dimensional multiferroic. The study was performed by using the Monte Carlo simulation. We applied the ANNNI Ising model for a one-dimensional multiferroic and the periodic Frenkel–Kontorova potential [20] to simulate the effect of the substrate. We found that the substrate significantly affects the structural changes near the magnetic phase transition temperature and reduces the polarization of the multiferroic at low temperatures.

2. Materials and Methods

We considered a model with competing FM nearest neighbor interactions J_{FM} and AFM next neighbor interactions J_{AF}. The distance dependencies of the FM and AFM exchange integrals can be presented as linear approximations [21]:

$$J_{FM}(r_{i,i+1}) = J_{FM_0} exp\left(\eta \frac{r_{i,i+1} - r_0}{r_0}\right) \approx J_{FM_0}\left(1 + \eta \frac{r_{i,i+1} - r_0}{r_0}\right) = J_{FM_0}[1 + \eta(d_{i+1} - d_i)] \tag{1}$$

$$J_{AF}(r_{i,i+2}) = J_{AF_0} exp\left(\eta \frac{r_{i,i+2} - 2r_0}{2r_0}\right) = J_{AF_0}\left[1 + \frac{\eta}{4}(d_{i+2} - d_i)\right], \tag{2}$$

where J_{FM_0} and J_{AF_0} are the FM and AFM exchange integrals in the absence magnetostriction, ($J_{FM_0} > 0$, $J_{AF_0} < 0$), r_0 is the interatomic distance in the ground state, η is the magnetostriction coefficient ($\eta < 0$), r_{ij} is the distance between i and $j = i+1, i+2$ ions, and d_i is the displacement of the i-ion from the initial position normalized to r_0.

To simplify the simulation, we will assume that only every even ion in the chain moves. This is true for chains with alternating atoms of two types. The magnitude of the AFM interaction for various atoms will be different due to the various magnetic moments. We take the relative values of magnetic moments for the $CoMnO_6$ chain, where the magnetic moment of Mn ions is three times larger than the magnetic moment of Co, i.e., ($J_{AF_{Mn}} = 9J_{AF_{Co}}$) [13]. The Mn ions are taken as immobile ($d_{Mn} = 0$). We use the periodic Frenkel–Kontorova potential to model the substrate influence. Then the Hamiltonian is:

$$H = H_{FM} + H_{AF} + H_M + H_E + H_{el} + H_{FK} \tag{3}$$

$$H_{FM} = -\sum_{\langle i,j \rangle} J_{FM}(r_{i,j})S_iS_j; \quad H_{AF} = -\sum_{[i,k]}^{Mn} J_{AF_{Mn}}S_iS_j - \sum_{[i,k]}^{Co} J_{AF_{Co}}(r_{i,j})S_iS_j;$$

$$H_M = -hg\mu_B \sum_i S_i; \quad H_E = -E\sum_i qd_i; \quad H_{el} = \frac{1}{2}k\sum_i d_i^2;$$

$$H_{FK} = -\alpha_{FK}\sum_i cos\left(\frac{2\pi(i + d_i)}{b_{FK}}\right),$$

where H_{FM} and H_{AF} are the competing FM and AFM interactions, the angle brackets denote the summation over the pairs of nearest neighbors, and the square brackets denote the summation over pairs of next-nearest neighbors. H_M and H_E are the energies of the magnetic and electric fields, respectively, h is the external magnetic field, g is the Landé factor, μ_B is the Bohr magneton, E is the external electric field, and q is the charge of moving ions ($q = 2$ for Co). H_{el} is the elastic energy, where k is the elasticity coefficient, H_{FK} describes the periodic potential of the substrate, α_{FK} and b_{FK} are the amplitude and the period of the potential. We take the Boltzmann constant as a unit, so the temperature is measured in units of energy.

The simulation parameters are presented in Table 1. We selected them to provide the qualitative agreement with experiment [13].

Table 1. The simulation parameters.

Parameter	Value	Parameter	Value
J_{FM_0}	360	η	−8
$J_{AF_{Mn}}$	−262.8	k	136,000
$J_{AF_{Co_0}}$	−29.2	g	2

The simulation was carried out on a chain of length $L = 4000$ with periodic boundary conditions. For each temperature value, the system came to the state of thermodynamic equilibrium during 3×10^5 Monte Carlo (MC) steps. Thermodynamic parameters were calculated during the next 5×10^4 MC steps.

The electrical susceptibility of a chain was calculated according to the statistical fluctuation [22]:

$$\chi_e = \frac{\langle P^2 \rangle - \langle P \rangle^2}{T}. \tag{4}$$

The dielectric constant is determined as:

$$\varepsilon = \chi_e + 1. \tag{5}$$

3. Results

Figure 1 shows the calculated temperature dependencies of the polarization P (Figure 1a), magnetic susceptibility ($\chi = M/h$) (Figure 1b), permittivity ε (Figure 1c) without the substrate influence, and the corresponding experimental curves for $Ca_3Co_{2-x}Mn_xO_6$ ($x = 0.96$) [22]. A comparison of simulation results with experimental data indicates their qualitative agreement.
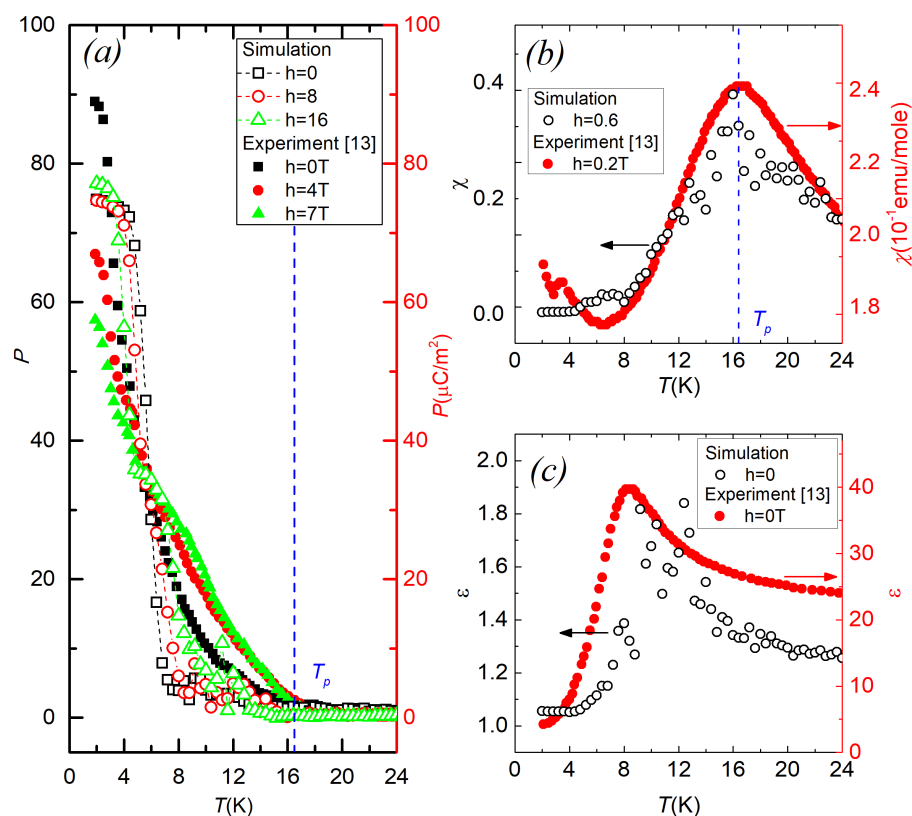
Figure 1. Temperature dependencies of polarization (**a**), magnetic susceptibility (**b**), and permittivity (**c**) were obtained from the simulation (opened symbols) and the experiment (filled symbols) [13].

The broad peak of the $\chi(T)$ indicates the presence of a phase transition from the AFM to the paramagnetic phase at $T_p \approx 16$. One can see the decrease in electric polarization below this temperature. The inclusion of a magnetic field reduces the polarization at $T < 6$ and increases it at a higher temperature. The experimental curves [13] demonstrate similar behavior and confirm the results of simulations.

Figure 2 shows the electric polarization change under the influence of the periodic potential of the substrate in the presence and the absence of an external magnetic field. We considered the cases when the period of the substrate potential was larger and smaller by 5% than the interatomic distance r_0. It can be seen that the substrate potential reduces the macroscopic polarization proportionally to the amplitude. However, the deviation of the potential period less or higher than the lattice constant reduces the polarization similarly.
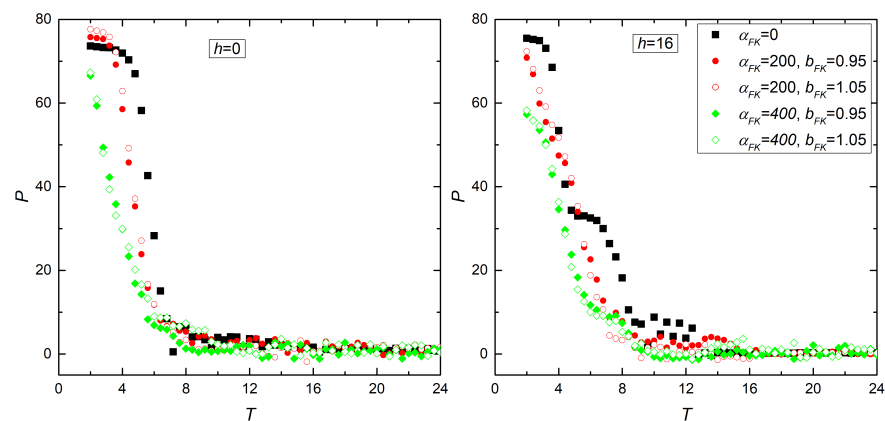

Figure 2. Temperature dependencies (unit: J_{FM_0}/k_B) of the polarization at the different periodic potentials of the substrate.

We analyzed the energy components by themselves for further study of the magnetic and electrical parameters of the system. We chose the FM and AFM interactions H_{FM} and H_{AF}, the influence energy of the substrate H_{FK}, and the elastic energy H_{el} as the main components.

Figure 3 shows the temperature dependencies of these components without and with the substrate when the period of the substrate potential is smaller (Figure 3(filled circles)) and larger (Figure 3(opened circles)) than the interatomic distance by 5%. The H_{FM} and H_{AF} dependencies have singularities at the transition temperature T_p, which indicates that the magnetic structure is destroyed. Note that T_p shifts slightly higher with a decrease in the potential period ($b_{FK} = 0.95$). Identical change in the phase transition temperature was observed for 2D magnets in [23]. At a temperature $T < 12$, H_{FM} and H_{AF} are almost the same in the presence and absence of the substrate potential. However, the dependencies of these components change dramatically at temperatures above 12. Near T_p, H_{FM} and H_{AF} change the type of extremum: a maximum instead of a minimum and vice versa. This indicates a change in the balance of FM/AFM interactions, i.e., toward the AFM interaction with the presence of the substrate potential and toward the FM interaction without it.

The behavior of H_{el} also changes with the substrate potential. Instead of a minimum at T_p in the absence of the potential, it demonstrates a maximum (Figure 3d). The H_{FK} energy has a minimum at T_p (Figure 3c), suggesting that a system has the minimum displacements at T_p without the substrate and the maximum displacements when the substrate appears. However, the growth of macroscopic polarization at T_p does not take place with the substrate potential (Figure 2). To explain this, let us consider the evolution of the magnetic subsystem in detail.
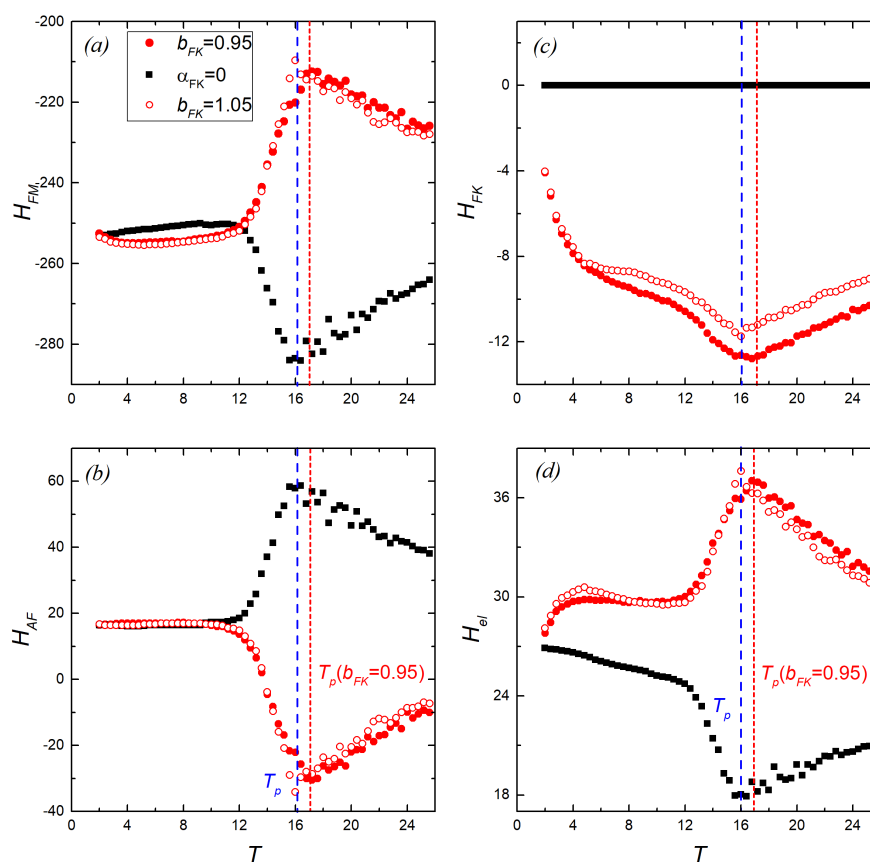
Figure 3. H_{FM} (**a**), H_{AF} (**b**), H_{FK} (**c**), and H_{el} (**d**) as functions of temperature (unit: J_{FM_0}/k_B) at different periodic substrate potentials (**circles**) and in its absence (**filled squares**). Note that $h = 0.6$.

Figure 4 shows the formation mechanism of microscopic polarization when the distances between parallel spins decrease and the distances between anti-parallel spins increase. The magnetic domain with an odd number of spins contributes to the formation of shifts in opposite directions (Figure 4b), thereby reducing the macroscopic polarization.
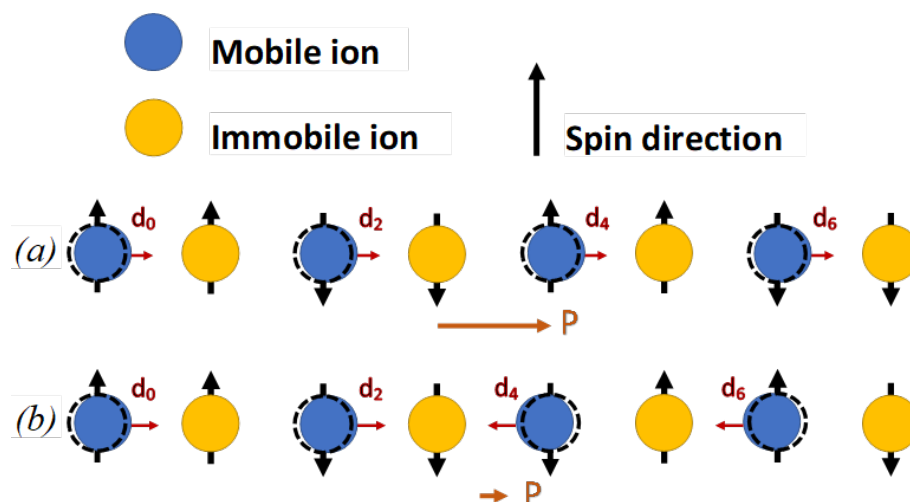
Figure 4. Formation of the electric polarization. Red arrows indicate ion displacements. (**a**) A chain with *up–up–down–down* ordering. (**b**) A magnetic domain of three spins lined in one direction results in oppositely directed displacements.

Therefore, we study the distribution of magnetic domains with even and odd numbers of spins. Let us consider the number of magnetic domains $N_d(n_s)$, where the length of magnetic domains n_s is the number of neighboring spins lined in one direction. Figure 5 shows the distribution of magnetic domains with $n_s = 2.5$ as the function of the temperature.

Figure 5a shows the case without substrate influence. At low temperatures ($T < 4$), the system contains domains with lengths of two and four spins, while there are no domains with lengths of three and five. In this region, the macroscopic polarization has a maximum. With an increase in temperature, domains with an odd number of spins appear, and there are fewer domains with an even number of spins. In this area, the polarization decreases (Figure 2). A significant decrease of $N_d(2)$ occurs near the phase transition temperature. The substrate potential lowers the temperature at which $N_d(3) \approx N_d(4) \approx N_d(5)$. The behavior of $N_d(2)$ with the substrate potential is very different at $T > 10$ (Figure 5b). It grows to T_p, and the number of domains with odd n_s increases near T_p.
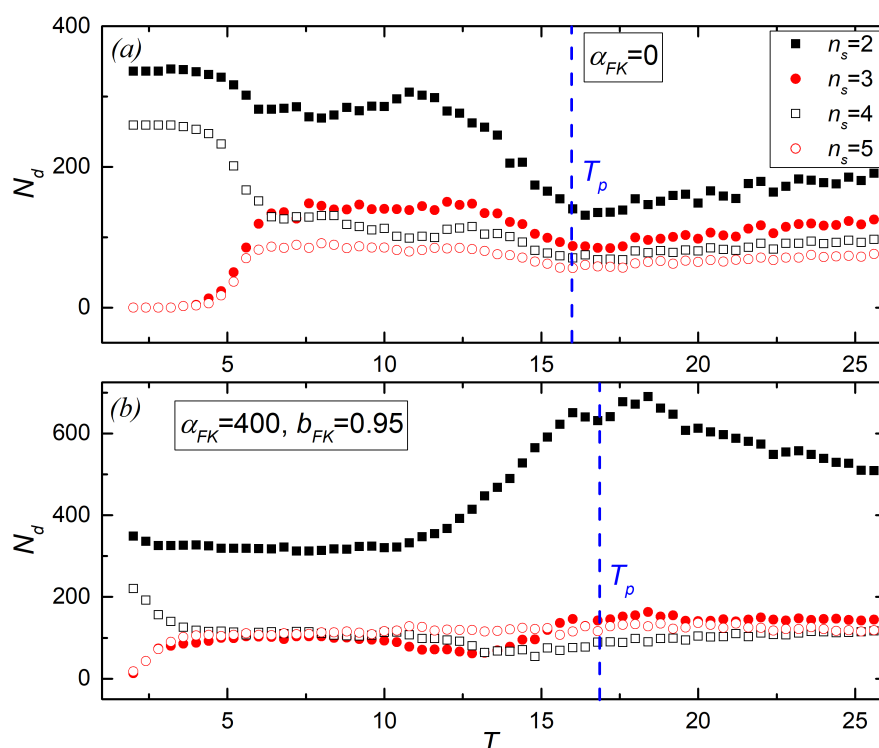
Figure 5. Number of magnetic domains with a length of 2 to 5 spins depending on temperature (unit: J_{FM_0}/k_B) (**a**) without the substrate potential and (**b**) in the presence of the substrate potential with an amplitude of 400 and a period of 0.95.

Figure 6 shows the distribution of N_d at different temperatures. Without substrate potential (Figure 6a), only domains with even n_s are present in the system at $T = 2$. The curve becomes smooth as the temperature rises, and domains with odd n_s appear. The substrate potential changes the behavior of N_d at higher temperatures. At $T = 10$, the number of domains with odd n_s increases, and it becomes higher than the number with even n_s. At $T = 15$, $N_d(2)$ increases significantly. This can be explained by the AFM interaction increase and the FM interaction decrease near T_p, as shown in Figure 3a,b. Thus, the polarization of the system does not increase significantly despite a visible increase of $N_d(2)$ near T_p. Displacements formed by magnetic domains with even n_s are compensated by oppositely directed displacements formed by domains with odd n_s.
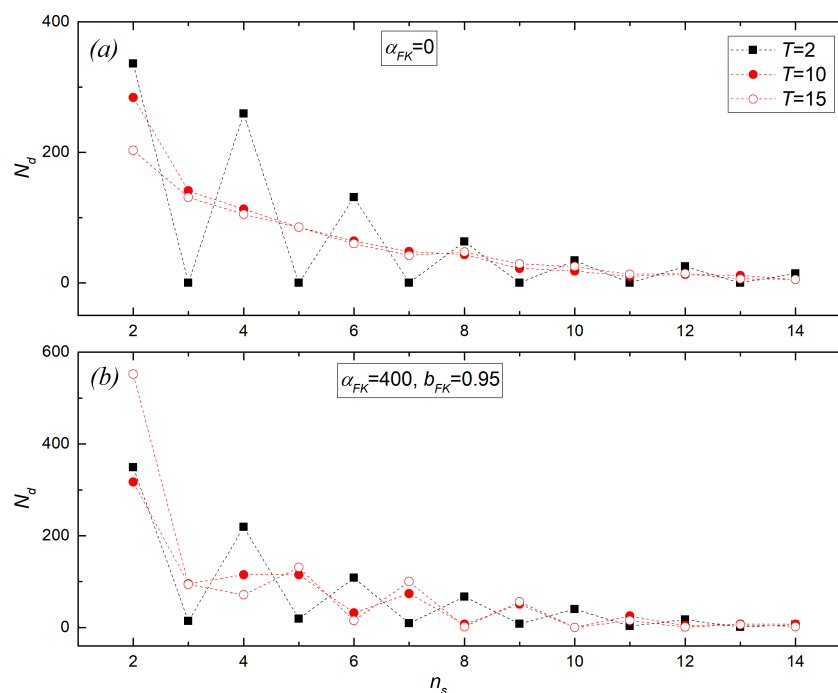
Figure 6. Number of magnetic domains at temperatures T = 2, 10, 15 (**a**) without the substrate potential and (**b**) in the presence of the substrate potential with an amplitude of 400 and a period of 0.95.

4. Conclusions

In this work, we studied the influence of the periodic substrate potential on the behavior of the thermodynamic parameters of a quasi-one-dimensional multiferroic. We investigated the case of a little deviation of the potential period from the interatomic distance in a spin chain of multiferroic. The discrepancy between the period of the substrate potential and the interatomic distance leads to a change in the space between atoms and, as a consequence, a change in the exchange integrals. The analysis of the individual energy components of the system showed a change in the balance of FM/AFM interactions when the substrate potential appeared. Near the magnetic phase transition, the AFM interaction starts to increase, while the FM interaction becomes weaker. The elastic component of the energy also changes its behavior when the substrate potential appears: the energy maximum appears instead of the minimum at the phase transition point. At this point, the displacements of spins from the equilibrium position are the largest. This leads to an increase in the number of magnetic domains with a length of two spins, which contributes to the creation of microscopic polarization, as well as domains with odd lengths, which contribute to the appearance of an oppositely directed polarization. As a result, macroscopic polarization does not change significantly.

Institutional Review Board Statement: Not applicable.

Informed Consent Statement: Not applicable.

Data Availability Statement: The data presented in this study are available upon request from the corresponding author.

Conflicts of Interest: The authors declare no conflict of interest.

References

1. Hu, M.; Li, S.; Wang, C. Substrate-imposed strain engineering of multiferroic properties in BCZT/LCMO bilayer heterostructures. *Appl. Surf. Sci.* **2020**, *509*, 145314. [CrossRef]
2. Odkhuu, D.; Kioussis, N. Strain-driven electric control of magnetization reversal at multiferroic interfaces. *Phys. Rev. B* **2018**, *97*, 094404. [CrossRef]
3. Panchal, G.; Choudhary, R.J.; Phase, D.M. Magnetic properties of $La_{0.7}Sr_{0.3}MnO_3$ film on ferroelectric $BaTiO_3$ substrate. *J. Magn. Magn. Mater.* **2018**, *448*, 262–265. [CrossRef]
4. Zubkov, V.; Bazuev, G.; Tyutyunnik, A.; Berger, I. Synthesis, Crystal Structure, and Magnetic Properties of Quasi-One-Dimensional Oxides Ca_3CuMnO_6 and $Ca_3Co_{1+x}Mn_{1-x}O_6$. *J. Solid State Chem.* **2001**, *160*, 293–301. [CrossRef]
5. Fjellvåg, H.; Gulbrandsen, E.; Aasland, S.; Olsen, A.; Hauback, B.C. Crystal Structure and Possible Charge Ordering in One-Dimensional $Ca_3Co_2O_6$. *J. Solid State Chem.* **1996**, *124*, 190–194. [CrossRef]
6. Hervoches, C.; Okamoto, H.; Kjekshus, A.; Fjellvåg, H.; Hauback, B. Crystal structure and magnetic properties of the solid-solution phase $Ca_3Co_{2-v}Mn_vO_6$. *J. Solid State Chem.* **2009**, *182*, 331–338. [CrossRef]
7. Khomskii, D. Classifying Multiferroics: Mechanisms and Effects. *Physics* **2009**, *2*, 20. [CrossRef]
8. van den Brink, J.; Khomskii, D.I. Multiferroicity due to charge ordering. *J. Phys. Condens. Matter* **2008**, *20*, 434217. [CrossRef]
9. Bellido, N.; Simon, C.; Maignan, A. Magnetodielectric coupling in $Ca_3Co_2O_6$ triangular Ising lattice. *J. Magn. Magn. Mater.* **2009**, *321*, 1770–1772. [CrossRef]
10. Fisher, M.E.; Selke, W. Infinitely Many Commensurate Phases in a Simple Ising Model. *Phys. Rev. Lett.* **1980**, *44*, 1502–1505. [CrossRef]
11. Wu, H.; Burnus, T.; Hu, Z.; Martin, C.; Maignan, A.; Cezar, J.C.; Tanaka, A.; Brookes, N.B.; Khomskii, D.I.; Tjeng, L.H. Ising Magnetism and Ferroelectricity in Ca_3CoMnO_6. *Phys. Rev. Lett.* **2009**, *102*, 026404. [CrossRef] [PubMed]
12. Zhang, Y.; Xiang, H.J.; Whangbo, M.H. Interplay between Jahn-Teller instability, uniaxial magnetism, and ferroelectricity in Ca_3CoMnO_6. *Phys. Rev. B* **2009**, *79*, 054432. [CrossRef]
13. Choi, Y.J.; Yi, H.T.; Lee, S.; Huang, Q.; Kiryukhin, V.; Cheong, S.W. Ferroelectricity in an Ising Chain Magnet. *Phys. Rev. Lett.* **2008**, *100*, 047601. [CrossRef] [PubMed]
14. Cabra, D.C.; Dobry, A.O.; Gazza, C.J.; Rossini, G.L. Topological solitons and bulk polarization switch in collinear type-II multiferroics. *Phys. Rev. B* **2021**, *103*, 144421. [CrossRef]
15. Ouyang, Z.W.; Xia, N.M.; Wu, Y.Y.; Sheng, S.S.; Chen, J.; Xia, Z.C.; Li, L.; Rao, G.H. Short-range ferromagnetic correlations in the spin-chain compound Ca_3CoMnO_6. *Phys. Rev. B* **2011**, *84*, 054435. [CrossRef]
16. Lin, L.; Guo, Y.J.; Xie, Y.L.; Dong, S.; Yan, Z.B.; Liu, J.M. Spin frustration destruction and ferroelectricity modulation in Ca_3CoMnO_6: Effects of Mn deficiency. *J. Appl. Phys.* **2012**, *111*, 07D901. [CrossRef]
17. Gong, G.; Zhou, J.; Duan, Y.; Hu, H.; Wang, Y.; Cheng, X.; Su, Y. Relaxor ferroelectric nature and magnetoelectric coupling of the one dimensional frustrated Ca_3CoMnO_6. *J. Alloys Compd.* **2022**, *908*, 164587. [CrossRef]
18. YE, Z.G.; BOKOV, A.A. Dielectric and Structural Properties of Relaxor Ferroelectrics. *Ferroelectrics* **2004**, *302*, 227–231. [CrossRef]
19. Pandya, R.J.; Zinzuvadiya, S.; Sengunthar, P.; Patel, S.S.; Thankachen, N.; Joshi, U. Microstructural, dielectric, magneto-electric and optical properties of single phase Ca_3CoMnO_6. *Phys. B Condens. Matter* **2021**, *601*, 412656. [CrossRef]
20. Frenkel, Y.; Kontorova, T. On the theory of plastic deformation and twinning. *Acad. Sci. USSR J. Phys.* **1939**, *1*, 137–149.
21. Yao, X.; Lo, V.C. Monte Carlo simulation of ferroelectricity induced by collinear magnetic order in Ising spin chain. *J. Appl. Phys.* **2008**, *104*, 083919. [CrossRef]
22. Privman, V. *Finite Size Scaling and Numerical Simulation of Statistical Systems*; World Scientific: Singapore, 1990.
23. Belim, S.V.; Bychkov, I.V.; Maltsev, I.; Kuzmin, D.A.; Shavrov, V.G. Tuning of 2D magnets Curie temperature via substrate. *J. Magn. Magn. Mater.* **2022**, *541*, 168553. [CrossRef]